Microenvironment and Immunology

PD-1 Blockade Enhances T-cell Migration to Tumors by Elevating IFN-γ Inducible Chemokines

Weiyi Peng[1], Chengwen Liu[1], Chunyu Xu[1], Yanyan Lou[1], Jieqing Chen[1], Yan Yang[1], Hideo Yagita[2], Willem W. Overwijk[1], Gregory Lizée[1], Laszlo Radvanyi[1], and Patrick Hwu[1]

Abstract

Adoptive cell transfer (ACT) is considered a promising modality for cancer treatment, but despite ongoing improvements, many patients do not experience clinical benefits. The tumor microenvironment is an important limiting factor in immunotherapy that has not been addressed fully in ACT treatments. In this study, we report that upregualtion of the immunosuppressive receptor programmed cell death-1 (PD-1) expressed on transferred T cells at the tumor site, in a murine model of ACT, compared with its expression on transferred T cells present in the peripheral blood and spleen. As PD-1 can attenuate T-cell–mediated antitumor responses, we tested whether its blockade with an anti–PD-1 antibody could enhance the antitumor activity of ACT in this model. Cotreatment with both agents increased the number of transferred T cells at the tumor site and also enhanced tumor regressions, compared with treatments with either agent alone. While anti–PD-1 did not reduce the number of immunosuppressive regulatory T cells and myeloid-derived suppressor cells present in tumor-bearing mice, we found that it increased expression of IFN-γ and CXCL10 at the tumor site. Bone marrow–transplant experiments using IFN-γR−/− mice implicated IFN-γ as a crucial nexus for controlling PD-1–mediated tumor infiltration by T cells. Taken together, our results imply that blocking the PD-1 pathway can increase IFN-γ at the tumor site, thereby increasing chemokine-dependent trafficking of immune cells into malignant disease sites. *Cancer Res; 72(20); 5209–18. ©2012 AACR.*

Introduction

The treatment of metastatic cancer with *ex vivo* activated T cells has been shown to result in tumor regression in a number of malignancies including melanoma, neuroblastoma, and lymphoma (1–3). However, as response rates are variable and complete responses remain infrequent, improvements to this approach are needed. One of the limitations to adoptive cell transfer (ACT) is obtaining adequate numbers of T cells which will ultimately migrate to and function at the tumor site. Indeed, we have found in metastatic melanoma patients that clinical response is strongly associated with the number of CD8+ T cells transferred (4), which may reflect a general lack of efficient T-cell migration to the tumor (5, 6). In addition,

inadequate persistence of transferred T cells and inhibition by the immunosuppressive tumor microenvironment likely also contribute to the lack of clinical responses observed in some patients (7, 8). To address these challenges, several strategies have been used to optimize the migration, survival and effector functions of transferred T cells within the tumor site, including transducing the chemokine receptor CXCR2 into T cells to improve migratory ability toward tumors (9), manipulating IL-2 production by transferred T cells to extend T-cell survival (10), and generating chimeric antigen receptor–based engineered T cells to improve recognition of tumor (11). However, all of these approaches could benefit from strategies that can reverse the immunosuppressive environment present at the tumor site.

Programmed cell death-1 (PD-1) is an inhibitory immune receptor on T cell that is expressed following T-cell activation. In the tumor microenvironment, PD-L1, the ligand for PD-1, can be upregulated on tumor cells and tumor-associated stromal cells (12). The engagement of PD-1 by PD-L1 or PD-L2, delivers inhibitory signals through activating phosphatases, resulting in dephosphorylation of key elements in the T-cell activation pathway. The dephosphorylation of these molecules leads to the inhibition of PI3K activity and downstream activation of Akt, which are important pathways in regulating proliferation, survival, and cytokine production of T cells (13). Activation of the PD-1 pathway is now recognized to be a major mechanism by which tumors suppress T-cell–mediated antitumor immune responses (14, 15).

In this study, we examined the role of the PD-1 pathway in the context of an ACT-based murine tumor treatment model.

Authors' Affiliations: [1]Department of Melanoma Medical Oncology, The Center for Cancer Immunology Research, The University of Texas MD Anderson Cancer Center, Houston, Texas; and [2]Department of Immunology, Juntendo University School of Medicine, Tokyo, Japan

Our results show that *in vivo* PD-1 blockade can increase the numbers of transferred T cells at the tumor site and enhance tumor regression in 2 tumor models. Furthermore, anti–PD-1 antibody appears to mediate these antitumor effects through augmented T-cell proliferation, in addition to increased IFN-γ and IFN-γ inducible chemokine production at the tumor site. Taken together, our study suggests that PD-1 blockade in combination with ACT shows therapeutic synergy, and provides a potential strategy for improving clinical response rates to ACT.

Materials and Methods

Animals and cell lines

Pmel-1 TCR/Thy1.1 transgenic mice on a C57BL/6 background were kindly provided by Dr. Nicholas Restifo (Surgery Branch, National Cancer Institute, Bethesda, MD). IFNγ receptor deficient mice and CXCL10 deficient mice were purchased from the Jackson Laboratory. All mice were maintained in a specific pathogen-free barrier facility at The University of Texas MD Anderson Cancer Center, Houston, TX. Mice were handled in accordance with protocols approved by the Institutional Animal Care and Use Committee. B16 melanoma and MC38 colon adenocarcinoma cells were obtained from the National Cancer Institute. The MC38/gp100 cell line was established as previously described (9). All tumor cell lines were maintained in RPMI 1640 with 10% fetal calf serum and 100 μg/mL Normocin (Invivogen).

Adoptive transfer, vaccination, and anti-PD-1 antibody treatment

Nine days before ACT, splenocytes from pmel-1 TCR/Thy1.1 transgenic mice were harvest and infected with a retroviral vector encoding a modified firefly luciferase gene and green fluorescent protein as previously described (9). After sorting based on green fluorescent protein expression, luciferase-expressing pmel-1 T cells were used for ACT. Wild-type (WT) or IFNγ receptor–deficient mice were subcutaneously implanted with either 5×10^5 B16 cells or 5×10^5 MC38/gp100 cells (day 0). On day 6, lymphopenia was induced by administering a nonmyeloablative dose (350 cGy) of radiation. On day 7, 1×10^6 luciferase-expressing pmel-1 T cells were adoptively transferred into tumor-bearing mice ($n = 3$–5 per group), followed by intravenous injection of 1×10^6 hgp100 peptide-pulsed bone marrow–derived dendritic cells (DC) generated as previous described (9). Recombinant human IL-2 was intraperitoneally administered for 3 d after T-cell transfer (1.2×10^6 IU once immediately after T-cell transfer and 6×10^5 IU twice daily for the next 2 days). Tumor sizes were monitored every 2 days. Mice were sacrificed when the tumors exceeded 15 mm in diameter or when ulcers exceeded 2 mm. All experiments were carried out in a blinded, randomized fashion.

The anti-mouse PD-1 antibody (RMP1–14) was prepared as described previously (16). For tumor treatment experiments, anti–PD-1 antibody or control rat IgG antibody (Sigma) was intraperitoneally injected starting on the day of T-cell transfer and was continued 2 and 4 days after T-cell transfer. Dose per injection was 250 μg.

Generation of bone marrow chimera mice

8-week-old female either WT B6 or IFNγ receptor deficient mice were subjected to 1,000 rad irradiation. 24 hours later, these mice were treated to achieve hematopoietic and immunologic reconstitution with 2×10^7 bone marrow cells taken from B6, IFNγ receptor deficient mice, or CXCL10 deficient mice. Six weeks after bone marrow transfer, these mice were used for ACT experiments.

Tumor infiltration and activation marker analysis

B16 or MC38/gp100 tumor-bearing mice receiving ACT treatment as discussed in the previous section were sacrificed on day 6 after T-cell transfer. Single-cell suspensions from spleen and excised tumor were prepared using a standard method. Lymphocytes from tumor samples were enriched on a Ficoll gradient (Accurate Chemical & Scientific Corp.). These single-cell suspensions were stained for intracellular and extracellular protein markers of interest. For BrdUrd staining, mice were intraperitoneally treated with 200 uL of 10 mg/mL solution of BrdUrd (BD Biosciences) 24 hour before collecting tissue samples. Stained samples were run on a BD FACSCanto II.

Staining antibodies included anti-CD45, anti-CD8, anti-CD90.1, anti-PD-1, anti-IFN-γ, anti-CD11b, Annexin-V, anti-BrdUrd, anti-F4/80, anti-Ly6C, and anti-Gr-1 (BD Biosciences); anti-Foxp3 (eBioscience); and anti-CXCL10 (R&D Systems).

In vivo Bioluminescence Imaging

Before imaging, mice were anesthetized with isoflurane and i.p. injected with 100 μL of 20 mg/mL D-Luciferin (Xenogen Corp.). After 8 min, animals were imaged using an IVIS 200 system (Xenogen), according to the manufacturer's instructions. Living Image software (Xenogen) was used to analyze data. Regions of interest were manually selected and quantification was reported as the average photon flux within regions of interest. The bioluminescence signal detected was represented as photons/s/cm^2/sr.

Quantitative real-time PCR

Tumor tissues were disrupted by a rotor-stator homogenizer and followed by RNA isolation using RNeasy Mini Kit (Qiagen) according to the manufacturer's protocol. Total RNA was resuspended in diethyl pyrocarbonate treated water. cDNA synthesis was then carried out using a cloned avian myeloblastosis virus first-strand cDNA synthesis kit (Invitrogen). Real-time (RT-PCR) was carried out using a C1000 Thermal cycler (Bio-Rad), using the SYBR Green technology, in a total volume 15 μL. Primers for the chemokines and cytokines of interest are listed in Supplementary Table S1. Samples were normalized relative to actin transcript expression levels.

Statistical analysis

The data were represented as mean $\pm$ SEM. Comparisons of differences in continuous variables between 2 groups were done using Student t tests. Differences in tumor size and T-cell numbers among different treatments were evaluated by ANOVA repeated-measures function. P values are based on 2-tailed tests, with $P < 0.05$ considered statistically significant.

Results

PD-1 is upregulated on adoptively transferred tumor-infiltrating T cells

PD-1 has been shown to be upregulated on tumor-infiltrating T cells and has been correlated with T-cell dysfunction at the tumor site. To address whether PD-1 blockade could improve the effectiveness of ACT, we first analyzed the expression of PD-1 on transferred CD8$^+$ T cells in mice with or without 7-day-established B16 tumors. These mice were treated with adoptively transferred pmel-1 T cells that express a TCR specifically recognizing a B16 tumor antigen, the H-2D^b–restricted epitope of gp100, followed by gp100 peptide-pulsed DC vaccine and IL-2 administration, as previously described. In our previous study, the majority of transferred T cells were found to be localized within tumor sites 6 days after T-cell transfer. Both endogenous and transferred T-cells displayed increased PD-1 positivity at the tumor sites compared with T cells localized in the spleen (Fig. 1 and Supplementary Fig. S1). To test the effector functions of transferred T cells, we measured IFN-γ production by transferred T cells with or without antigen restimulation. Although some transferred T cells produced IFN—γ at the tumor site, the tumor-infiltrating T cells were largely refractory to restimulation with gp100 pulsed DC, compared with pmel-1 T cells isolated from the spleen (Fig. 1). These results suggested that the B16 tumor microenvironment could induce the expression of PD-1 on transferred tumor-specific T cells and impair their effector function, potentially limiting the therapeutic efficacy of these cells.

PD-1 blockade promotes tumor rejection by increasing the number of transferred T cells at the tumor site

To test the potential of PD-1 pathway blockade to improve the therapeutic effects of ACT, we used our previously described MC38/gp100 tumor model, which, unlike B16 melanoma, is devoid of pigmentation and therefore can be used for *in vivo* monitoring of luciferase transduced adoptively transferred T cells. In this setting, anti-PD-1 antibody was intraperitoneally injected on days 0, 2, and 4 following T-cell transfer (Fig. 2A). Six days after transferring luciferase-expressing pmel-1 T cells, mice receiving either control antibody or anti–PD-1 antibody were imaged to observe luciferase intensity at the tumor sites. As shown in Fig. 2B, mice treated with ACT and anti–PD-1 displayed stronger luciferase signal at the tumor site than mice treated with ACT and control antibody. The average luciferase activity in all mice ($n = 4$) from each group was quantified (Fig. 2C), showing that PD-1 blockade induced approximately 3-fold more transferred T cells at the tumor site compared with mice administered the control antibody.

To determine whether the addition of anti–PD-1 had any effect on the antitumor immune response, we treated MC38/gp100-bearing mice with 1×10^6 pmel-1 T cells, a dose that had only limited antitumor effects in our preliminary experiments (data not shown), along with anti–PD-1 or control antibody. The tumor growth rates in mice treated with anti–PD-1 antibody, ACT or combination of ACT with anti–PD-1 are shown in Fig. 2D. We consistently observed some antitumor activity in mice treated with anti–PD-1 antibody alone, whereas ACT alone exhibited little or no antitumor impact. However, when mice were treated with a combination of ACT and PD-1 blockade, tumor progression was significantly inhibited as compared with anti–PD-1 alone, and some regression was evident. We also evaluated the treatment effect of anti–PD-1 in the B16 melanoma tumor model. Although little antitumor effect was observed in mice treated with anti–PD-1 antibody alone, antitumor responses were enhanced with a combination of ACT and PD-1 blockade compared with either therapy given

Figure 1. The expression of PD-1 by transferred T cells at the tumor and spleen of mice receiving ACT treatment. Mice with or without 7-day established B16 tumor were transferred with cultured T cells from pmel-1 TCR/Thy1.1 transgenic mice. Six days after T-cell transfer, single cell suspensions were obtained from spleens and tumors and stimulated with gp100-peptide pulsed DC in the presence of Golgi stop for 4 hours. Lymphocytes with or without stimulation were evaluated by flow cytometry for PD-1 versus IFN-γ after gating on CD8$^+$ and Thy1.1$^+$. Number indicates the percentage of cells showing in each quadrant. The flow data was obtained from pooled lymphocyte samples from 5 mice in each group. Two independent studies showed similar results.
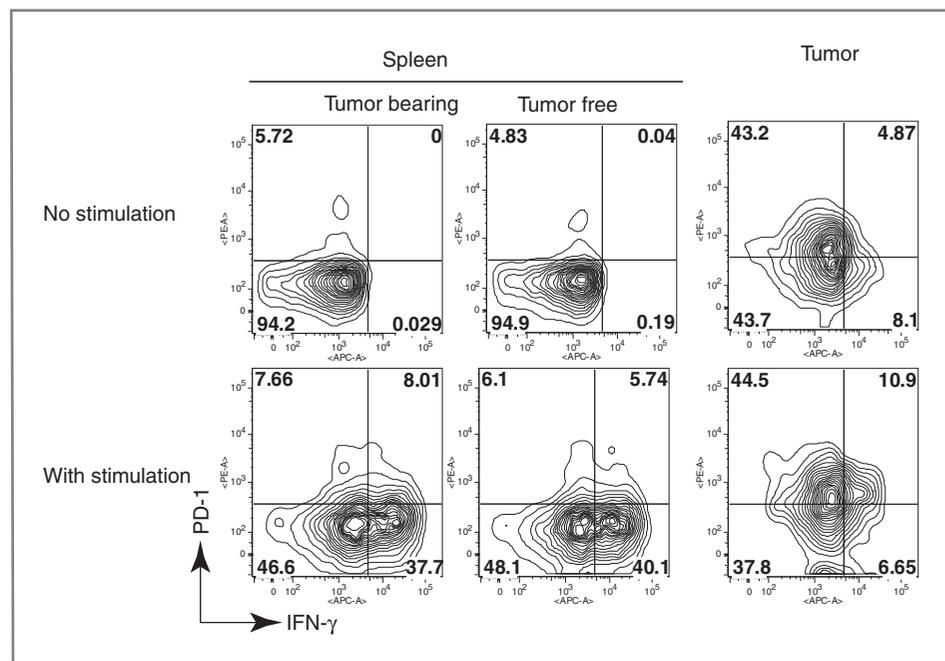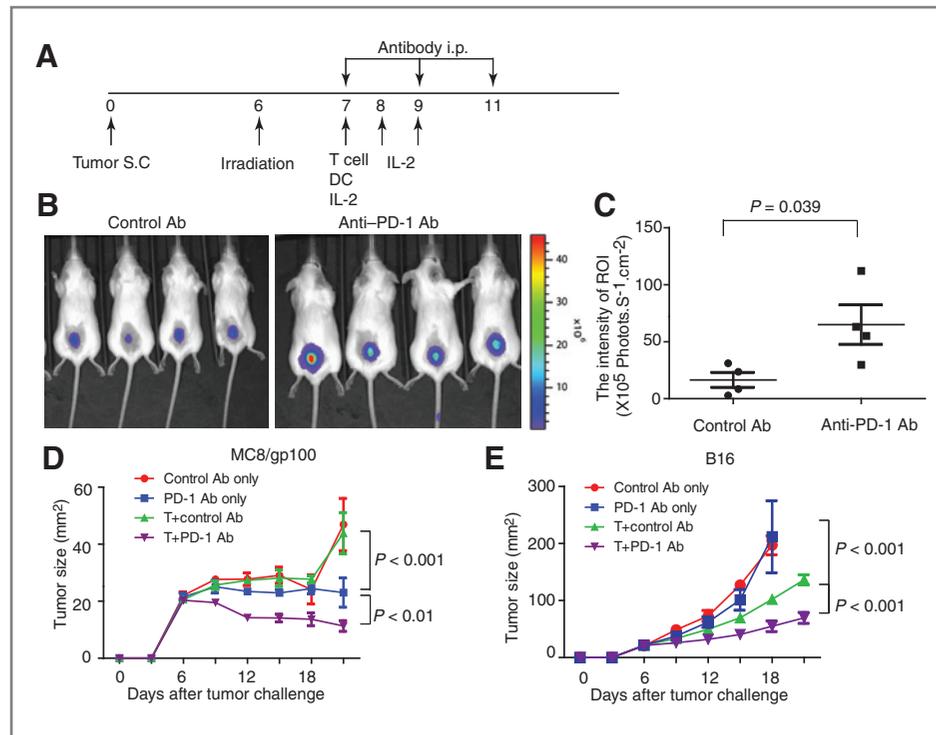
Figure 2. Increased accumulation of pmel-1 T cells to tumor sites and enhanced antitumor immune response in mice receiving ACT combined with anti-PD-1 antibody treatment. A, schematic representation of treatment schedule. B, *in vivo* trafficking of transferred pmel-1 T cells. Luciferase-expressing pmel-1 T cells (1×10^6) were transferred into mice bearing established 7-day MC38/gp100 tumors. DC vaccine and IL-2 treatment were conducted as previously described. Mice were intraperitoneally injected with 250 μg either control antibody or anti-PD-1 Ab on days 0, 2, and 4 after T-cell transfer. Imaging was conducted on day 6 after T-cell transfer. Data shown were from representative mice. C, quantitative imaging analysis of transferred T cells in tumor-bearing mice. Intensities of the luciferase signal at tumor sites in all tumor-bearing mice are depicted ($N = 4$ per group). D, tumor growth curve of MC38/gp100 tumor-bearing mice receiving anti–PD-1 Ab with or without adoptive T-cell transfer ($N = 5$ per group). E, tumor growth curve of B16 tumor-bearing mice receiving anti–PD-1 Ab with or without adoptive T-cell transfer ($N = 5$ per group).

alone (Fig. 2E). In both tumor models, mice tolerated the combined therapy with ACT and anti–PD-1 antibody with little evident toxicity. Hence, our results suggest that the addition of anti–PD-1 antibody could improve the therapeutic efficacy of ACT.

## PD-1 blockade enhances proliferation of transferred T cells at tumor sites

We next sought to determine the underlying mechanisms of improved antitumor responses observed with the combination therapy of ACT and PD-1 blockade by characterization of the phenotype of transferred T cells and other immunoregulatory cells at the tumor site. To avoid the potential alteration of the phenotype of immune cells caused by tumor digestion, we used the B16 tumor model, in which anti–PD-1 also shows an enhanced therapeutic effect in combination with ACT. Unlike many types of tumor tissue including MC38/gp100, a single cell suspension can be easily obtained by gentle mechanical disruption of B16 tumor tissue. B16-tumor-bearing mice were treated with ACT combined with anti–PD-1 antibody or control antibody as previously described, and the percentage and phenotypes of transferred pmel-1 T cells in the tumor and spleen were analyzed by flow cytometry on day 6 after T-cell transfer. Consistent with the results seen in MC38/gp100 tumor-bearing mice, in B16-bearing mice receiving anti–PD-

1 antibody, there were more pmel-1 tumor-infiltrating T cells (∼50%) compared with pmel-1 T cells in mice receiving a control antibody (∼20%, $P = 0.027$; Fig. 3A). Among mice pretreated with BrdUrd, we also found increased percentages of IFN-γ^+ and BrdUrd$^+$ cells in tumor-infiltrating CD8$^+$ T cells in the anti–PD-1 group when compared with the control antibody group, suggesting an enhanced proliferative ability of transferred T cells within the tumor. However, anti–PD-1 antibody failed to alter the percentages of tumor-infiltrating CCR7$^+$ cells, or Annexin$^+$ 7AAD$^+$ cells in pmel-1 T cells (Fig. 3A and B). Moreover, PD-1 blockade had little impact on the number and function of transferred T cells within the spleen. We also assessed the effect of the combination of ACT and anti–PD-1 treatment on immunosuppressive cell subsets within tumors, including regulatory T cells (T$_{reg}$) and myeloid-derived suppressor cells (MDSC). In contrast to the results of other studies (17), in our ACT model, we did not find alterations in the numbers of T$_{reg}$s or MDSCs in the tumor following anti–PD-1 antibody treatment (Supplementary Fig. S2).

ACT combined with PD-1 blockade upregulates CXCL10 expression in the tumor microenvironment

Given the important roles of chemokines in tissue trafficking and recruitment of lymphocytes, we next examined the

Figure 3. The phenotype and function of transferred pmel-1 T cells in mice receiving ACT and anti–PD-1 Ab treatment. A, change of frequency and function of transferred pmel-1 T cells within tumor and spleen in response to PD-1 blockade. Six days after T-cell transfer, B16-bearing mice were intraperitoneally treated with BrdUrd solution. Twenty-four hours later, mice were sacrificed to harvest tumor tissue and spleen ($N = 3$ per group). Single cell suspension was made from tumor and spleen and stained with anti-CD8, anti-Thy1.1, anti-CCR7, anti-IFN-γ, and anti-BrdUrd. B, apoptosis of transferred pmel-1 T cells at the tumor site. Six days after T-cell transfer, lymphocytes from tumor tissues were stained with anti-CD8, anti-Thy1.1, Annexin V, and 7AAD. Representative contour plots for 1 tissue sample from mice treated with ACT and anti–PD-1, as well as 1 tissue sample from mice treated with ACT with control antibody, are shown after gating with anti-Thy1.1^{+} and anti-CD8^{+} subsets. Values in each quadrant indicate the percentage of cells in the corresponding quadrant. (*, $P < 0.05$).
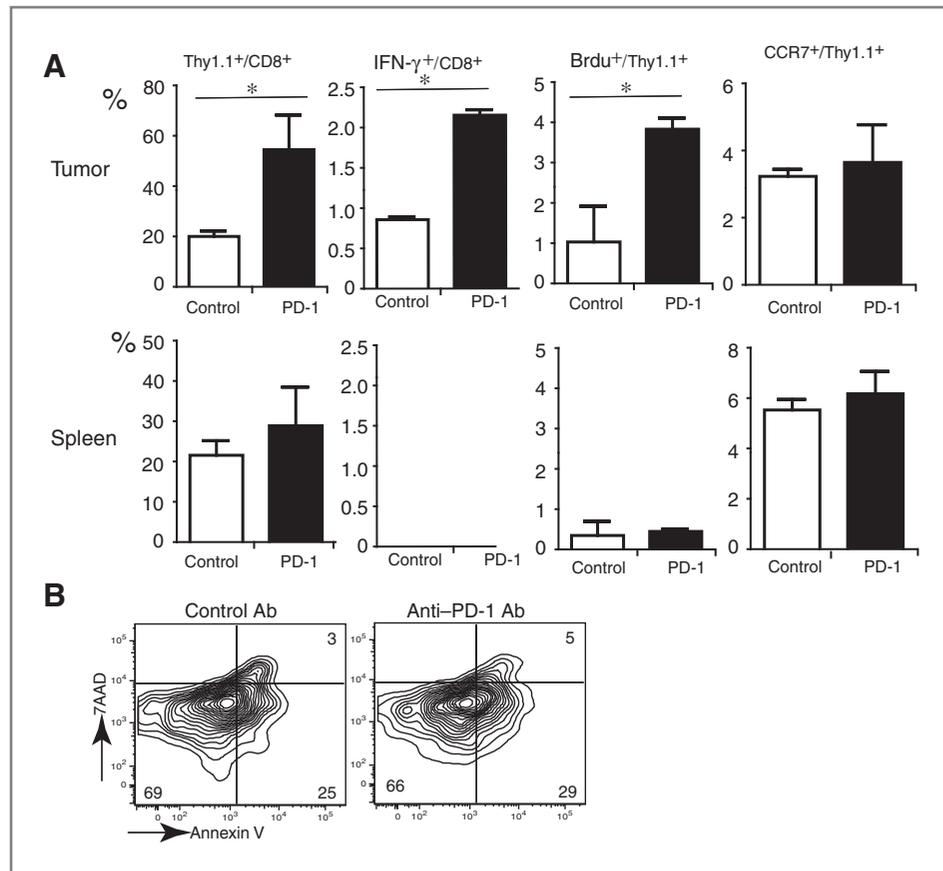
expression of 37 known murine chemokines within the tumor on day 6 after T-cell transfer using quantitative RT-PCR. With the exception of CCL6, 8, 19, and CXCL10, chemokines were generally expressed at low levels within tumors (Fig. 4A). However, in mice receiving the combination therapy of ACT and anti–PD-1, CXCL10 expression was significantly elevated compared with mice treated only with ACT (Fig. 4A). Using flow cytometry to analyze the CXCL10 production in the tumor microenvironment, we found that most of the CXCL10-secreting cells expressed CD11b, indicating that myeloid cells are the major CXCL10-producing population (Fig. 4B). These CXCL10-producing cells also express Gr-1 and Ly6C, but not or low F4/80, a macrophage surface marker (Supplementary Fig. S3). We also found that the percentage of CXCL10-producing cells at the tumor site from mice treated with ACT and anti–PD-1 was higher than that of mice treated with ACT and control antibody (Fig. 4C and D). However, the percentage of CXCL10-producing cells in the spleen from mice receiving ACT and anti–PD-1 Ab were similar to that of mice treated with ACT and control Ab (Supplementary Figure S4A). This data validated the results obtained by quantitative PCR and indicated that PD-1 blockade can enhance the expression of CXCL10 at the tumor site in mice receiving ACT. Because CXCL10 is an IFN-γ inducible chemokine, we also assessed the level of IFN-γ present within the tumor microenvironment. We indeed found increased IFN-γ levels within the tumors of mice undergoing combination therapy of ACT and anti–PD-1 compared with mice treated

with ACT alone (Fig. 4E). No significant difference in the expression of other cytokines was observed between treatment groups, including IL-10, TGF-β, and IL-17.

IFN-γ receptor is required for enhanced T-cell accumulation induced by PD-1 blockade

Our results suggested that PD-1 blockade might increase IFN-γ levels in the tumor microenvironment by enhancing the proliferation of transferred T cells, leading to increased CXCL10 production and the recruitment of more tumor-reactive T cells. To test this hypothesis, we challenged IFN-γ receptor deficient mice with B16 tumors, after which mice were treated with ACT with either anti–PD-1 antibody or control antibody. As shown in Fig. 5A, the percentage of transferred pmel-1 T cells in tumors from IFN-γ receptor–deficient mice treated with ACT and anti–PD-1 was not significantly different from that of IFN-γ receptor-deficient mice treated with ACT alone. In contrast, tumor-bearing WT mice treated with ACT and PD-1 blockade showed elevated percentages of transferred T cells within the tumor. As we found that the majority of CXCL10-producing cells in the tumor were CD11b^{+}, we next evaluated the importance of IFN-γ receptor expression on bone marrow–derived cells. IFN-γ receptor–deficient host mice were lethally irradiated and reconstituted with bone marrow cells from WT or IFN-γ receptor KO mice. Eight weeks later, these mice were challenged with tumor, treated with ACT combined with either
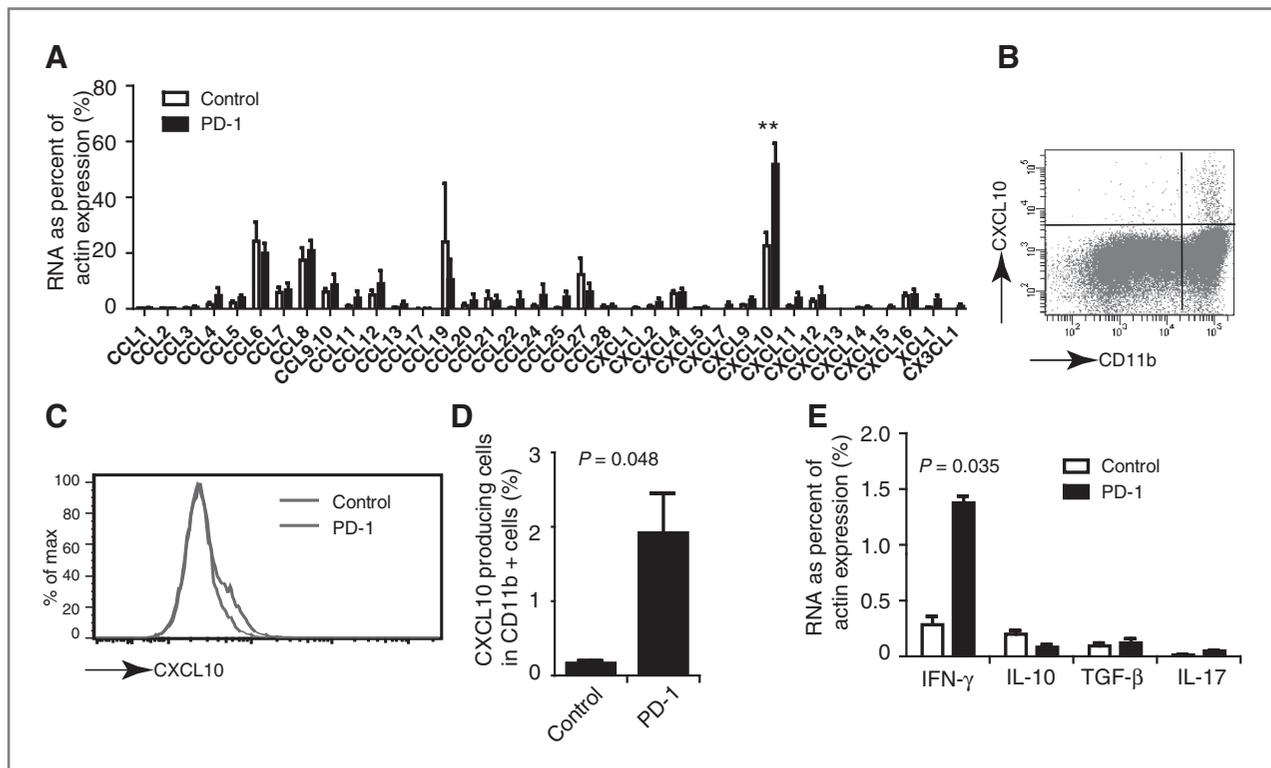
Figure 4. Change in chemokine and cytokine expression within tumors from mice receiving ACT in response to PD-1 blockade. A, chemokine mRNA levels within the tumor site from mice infused with pmel-1 T cells with or without PD-1 blockade. Mice challenged with 5×10^5 B16 cells received pmel-1 T cells on day 7, then treated with either anti–PD-1 antibody or control antibody on days 7, 9, and 11 and sacrificed on day 13. RNA was isolated from the tumor tissues of mice ($N = 3$ for each group). The expression levels of chemokine within tumors were analyzed by RT–PCR. B, representative plot of CXCL10-producing cells within tumor tissue. C, representative histogram plots of CXCL10 production within tumor tissue from mice treated with ACT and anti–PD-1, as well as from mice treated with ACT with control antibody, are shown after gating with CD11b$^+$ subsets. D, percentage of CXCL10-producing cells in CD11b$^+$ cells within tumor tissue from mice treated with ACT and anti–PD-1 as well as from mice treated with ACT with control antibody ($N = 3$–5 per group). E, cytokine mRNA levels within the tumor site from mice infused with pmel-1 T cells with or without PD-1 blockade. (**, $P < 0.01$).

anti–PD-1 or control antibody, then analyzed by flow cytometry to determine the number of transferred T cells localized to tumor. As shown in Fig. 5B, anti–PD-1 enhanced the number of pmel-1 T cells in the tumors of IFN-γ receptor–deficient mice reconstituted with bone marrow from WT mice, but not in mice reconstituted with bone marrow from IFN-γ receptor KO mice.

To determine the role of CXCL10, WT mice were reconstituted with bone marrow from CXCL10-deficient mice, challenged with tumor, treated by adoptive transfer with luciferase-expressing pmel-1 T cells. Six days following ACT, anti–PD-1 treatment led to increased luciferase intensity at the tumor site in mice reconstituted with bone marrow from WT mice, but not in mice reconstituted with bone marrow from CXCL10 deficient mice, similar to the results observed with IFN-γ receptor bone marrow donors. Most importantly, the addition of anti–PD-1 only significantly delayed tumor growth in mice reconstituted with bone marrow from WT mice, compared with ACT treatment alone (Fig. 5C). In contrast, the tumor growth rates in mice reconstituted with IFN-γ receptor deficient bone marrow or CXCL10-deficient bone marrow receiving ACT and anti–PD-1 were comparable with those in similar bone marrow chimeras treated with ACT alone (Fig. 5C). By using imaging to monitor transferred luciferase-transduced pmel-1 T cells in tumor-bearing mice on day 6 after ACT

treatment, we found that anti–PD-1 enhanced luciferase signal intensity at the tumor site in bone marrow chimera mice reconstituted with WT bone marrow, but not in the mice reconstituted with IFN-γ receptor deficient bone marrow or CXCL10-deficient bone marrow (Fig. 6). These results suggest that the IFN-γ inducible chemokine, CXCL10, plays a critical role in the synergistic antitumor effect observed in the combination therapy of anti–PD-1 with ACT. Moreover, in the chimeric mice reconstituted with CXCL10 deficient bone marrow, anti–PD-1 treatment resulted in a 2-fold increase of luciferase intensity at the tumor site, although the difference was not statistically significant. This suggests that other IFN-γ inducible chemokines may also play a role in the synergistic effect of anti–PD-1 on ACT.

Taken together, our study implies that blockade of the PD-1 pathway in T cells may trigger a positive feedback loop at the tumor site, increasing T-cell proliferation and IFN-γ levels, which in turn augments CXCL10 production by bone marrow–derived cells to enhance infiltration by effector T cells.

Discussion

PD-1 was first discovered as a transmembrane protein that is highly expressed in apoptotic T cells (18). In mice with viral
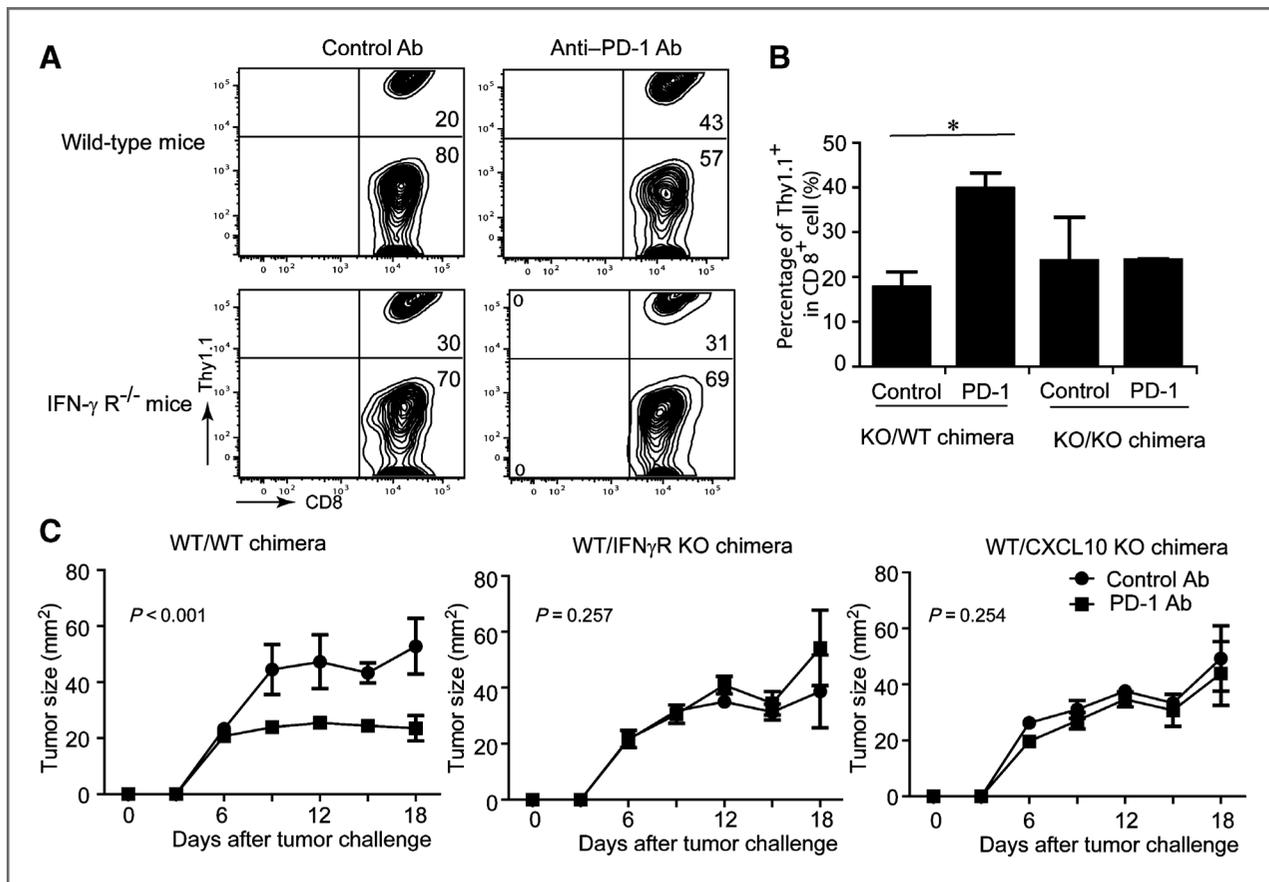
Figure 5. Failure to enhance antitumor immune response by anti–PD-1 antibody in mice with IFN-γ receptor–deficient or CXCL10 deficient in bone marrow–derived cells receiving ACT therapy. A, frequency of Thy1.1$^+$ in CD8$^+$ cells within the tumor site in IFN-γ receptor–deficient mice treated with ACT. WT or IFN-γ receptor–deficient mice were challenged with 5×10^5 tumor cells and infused with pmel-1 T cells on day 7, treated with either anti–PD-1 antibody or control antibody on days 7, 9, and 11, and then sacrificed on day 13. Single cell suspensions were made from tumor and stained with anti-CD8, anti-Thy1.1. Data shown were from representative mice. B, frequency of Thy1.1$^+$ in CD8$^+$ cells within the tumor site in bone marrow chimera mice treated with ACT. IFN-γ receptor–deficient mice received bone marrow either from WT mice or IFN-γ receptor–deficient mice 16 hours after 1,000 rad irradiation. Eight weeks after bone marrow transfer, the bone marrow chimera mice were challenged with tumor and received pmel-1 T cell as previously described. Anti–PD-1 or control antibody was intraperitoneally injected on days 0, 2, and 4 after T-cell transfer. The percentage of transferred pmel-1 T cells at the tumor site was analyzed on day 6 after T-cell transfer. C, tumor growth curve of MC38/gp100 tumor-bearing bone marrow chimera mice receiving ACT with control Ab or anti–PD-1 antibody ($N = 3$ for each group). WT female mice received bone marrow from WT mice, IFN-γ receptor–deficient mice, or CXCL10-deficient mice. Eight weeks after bone marrow transfer, the bone marrow chimera mice were challenged with MC38/gp100 tumor and received pmel-1 T cell as previously described.

infections, PD-1 was identified as a marker for exhausted T cells, and blockade of the PD-1 pathway restored cytokine production and increased the number of virus-specific T cells. More importantly, the viral load in infected mice was significantly reduced by inhibiting the PD-1 pathway (19). These results were later confirmed in human chronic viral infections: several studies found that human immunodeficiency virus (HIV)-specific T cells displayed an exhausted phenotype induced by chronic HIV viral infection and the expression of PD-1 on these cells was upregulated. A correlation between PD-1 expression on T cells and disease progression was found in HIV patients without therapy (20, 21). Furthermore, in humans with acute cytomegalovirus (CMV) infection, CMV-specific T cells had intact antiviral effector functions that correlated with lower levels of PD-1. In addition, PD-1–deficient mice spontaneously develop autoimmune diseases, including lupus-like

glomerulonephritis, arthritis, and diabetes (22, 23). These studies not only showed the important role of PD-1 in antiviral T-cell–mediated immunity, but also suggested that the interaction of PD-1 and its 2 ligands, PD-L1 or PD-L2, can deliver negative signals to regulate the function of T cells.

Subsequent studies confirmed that PD-1 is also an immune suppressive checkpoint molecule that tumors frequently exploit to modulate the function of tumor-infiltrating T cells. PD-1 has been shown to be upregulated on tumor-infiltrating T cells in patients with melanoma, renal cell carcinoma, and non–small cell lung cancer (24–27). In addition, PD-L1 and PL-L2 have been found to be expressed in numerous solid tumors and hematologic malignancies. Recent studies have shown a strong correlation between PD-1 ligand expression on tumor cells and poor prognosis in various cancers, including renal cell carcinoma, pancreatic cancer, cervical carcinoma, and
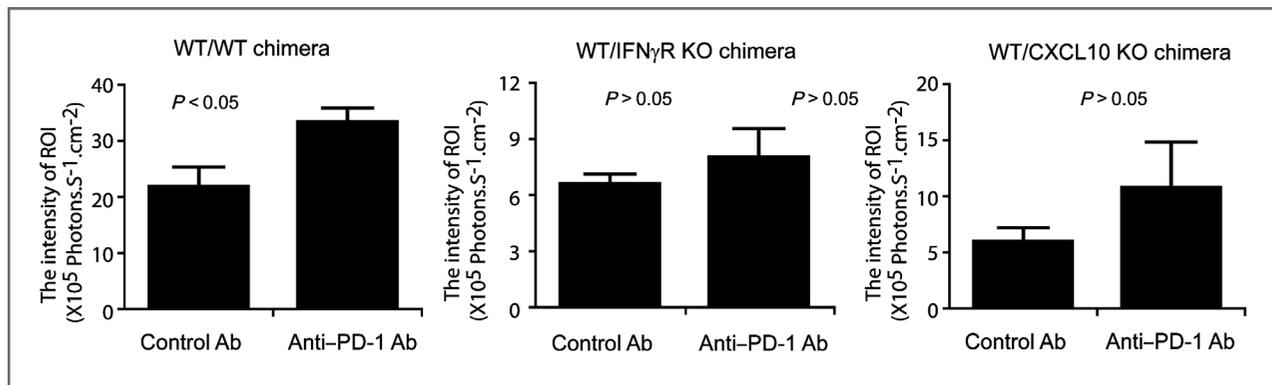
Figure 6. Failure to increase accumulation of pmel-1 T cells to tumor sites by anti–PD-1 in mice with IFN-γ receptor deficient or CXCL10 deficient in bone marrow-derived cells receiving ACT therapy. Bone marrow chimera mice ($N = 3$ for each group) were challenged with MC38/gp100 tumor and transferred with luciferase expressing pmel-1 T cells. Mice were intraperitoneally injected with either 250 μg control antibody or anti–PD-1 Ab on days 0, 2, and 4 after T-cell transfer. In vivo luciferase imaging was conducted on day 6 after T-cell transfer. Intensities of the luciferase signal at tumor sites in all tumor-bearing mice are depicted.

melanoma (28–31). Blocking the PD-1 pathway *in vivo* can restore defective effector function of tumor-infiltrating T cells. (14, 32) These results suggest that PD-1 ligands expressed within the tumor microenvironment may suppress T-cell–mediated antitumor immune responses by engaging PD-1 on tumor-infiltrating T cells.

Given the significance of PD-1 in modulating antitumor immunity, 2 monoclonal antibodies against PD-1, MDX-1106, and CT-011 have been tested in Phase I clinical trials to treat patients with cancer or hepatitis C viral infection. In a trial involving 32 cancer patients, MDX-1106 treatment induced 1 complete response, 2 partial responses and 2 mixed responses (33). More recently, objective responses by using MDX-1106 were also reported in patients with non-small-cell lung cancer, melanoma or renal-cell cancer (34). Six patients with advanced hematologic malignancies treated with CT-011 showed a 33% response rate with 1 patient experiencing a complete response (35). Although there were some rare but significant toxicities observed in all 3 clinical trials, their results showed that anti–PD-1 blocking antibodies are relatively safe compared with other immunotherapies, and well tolerated in the majority of cancer patients (33–35). However, the relatively low complete response rate observed with anti-PD-1 antibodies as a single-agent therapy highlights the importance of combining PD-1 blockade with other therapeutic agents. It was reported that combination blockade of PD-1 and CTLA-4 results in reduced numbers of regulatory T cells and myeloid cells at tumor sites and synergistically enhances the antitumor activity of effector T cells (17). Recently, several studies have tested the potential benefit of combining PD-1 blockade with tumor vaccines. Anti–PD-1 blocking antibody treatment combined with cyclo-phosphamide and peptide vaccine, led to complete tumor regression in tumor-bearing mice. In this model, anti–PD-1 was found to prolong the inhibition of T_{reg} functions at the tumor site induced by low dose cyclophosphamide (36). Similar delayed tumor progression was observed in mice treated with combination therapy of PD-1 blockade and lentiviral vaccine expressing trp2 tumor antigen, when compared with mice treated with PD-1 blockade or vaccine alone (37). Cancer

progression is regulated by the dynamic balance between antitumor immunity and immunosuppressive factors within the tumor microenvironment. ACT and PD-1 blockade shift this balance toward antitumor immunity using 2 distinct but complementary mechanisms. As PD-1 expression by T cells is frequently upregulated at tumor sites, we hypothesized that anti-PD-1 treatment might provide therapeutic synergy when combined with ACT. We found using 2 different mouse tumor models that anti–PD-1 blocking antibody can enhance the numbers of transferred T cells at tumor sites, resulting in delayed tumor progression. Furthermore, we found that while blockade of the PD-1 pathway had no impact on the apoptosis of transferred tumor-specific T cells in tumors, it modestly enhanced their proliferation, consistent with previous studies (38). Unlike the results from recently published studies, we did not find increased numbers of T_{reg} and MDSCs at the tumor site in response to anti–PD-1 antibody treatment. One possible reason is that the lymphodepletion procedure used in our ACT protocol may abolish the additional effects of anti–PD-1 antibody on T_{reg} and MDSC by transiently depleting these 2 cell subsets (17).

Unlike *in vitro* expanded human tumor-infiltrating T cells, which can be present in peripheral blood up to 1 year after T-cell transfer in our ACT clinical trial patients (39), *in vitro* expanded pmel-1 T cells are typically undetectable in the peripheral blood by day 9 after T-cell transfer and by day 13 at the tumor site (data not shown and Supplementary Fig. S4B). This suggests that this murine ACT model may not entirely mimic the clinical setting in patients with ACT, particularly with regard to T-cell persistence. Although we did not observe extended persistence of these transferred T cells in our murine ACT model, further clinical studies in patients are required to evaluate the effect of anti–PD-1 on the persistence of transferred T cells and survival of patients treated with ACT.

Our results also showed that IFN-γ signaling is critical for the enhanced accumulation of T cells at the tumor site. Blockade of the PD-1 pathway appeared to generate increased IFN-γ and the IFN-γ inducible chemokine CXCL10, as CXCL10

was present at increased levels in the tumor microenvironment following anti–PD-1 treatment. Although CXCL10 is secreted by various cell types, including neutrophils, monocytes, and dendritic cells, we found that CD11b$^+$ myeloid cells were the major source of CXCL10 at the tumor site (40). Characterization of these CXCL10-producing cells indicated that these cells share some common markers of myeloid-derived suppressor cells (MDSCs), but do not express the F4/80 macrophage marker, which are consistent with the phenotype of granulocytic MDSCs. Furthermore, anti–PD-1 treatment enhanced the percentage of CXCL10-producing CD11b$^+$ cells at the tumor site compared with mice given ACT alone. These results imply that anti–PD-1 treatment may tilt the balance in favor of a T-cell mediated antitumor immune response in ACT by altering the function of MDSCs, an immunosuppressive cell subset within the tumor microenvironment.

Taken together, our results implied that blockade of the PD-1 pathway may trigger a positive feedback loop by increasing IFN-γ presence at the tumor site and inducing CXCL10 production, to further improve the antitumor efficacy of ACT. Given the synergistic impact of anti–PD-1 on the therapeutic efficacy of ACT, combination therapies utilizing PD-1 blockade and ACT may represent a promising dual immunotherapy for cancer patients.

Authors' Contributions

Conception and design: W. Peng, C. Liu, P. Hwu
Development of methodology: W. Peng, C. Liu, H. Yagita, W.W. Overwijk, L. Radvanyi
Acquisition of data (provided animals, acquired and managed patients, provided facilities, etc.): W. Peng, C. Xu, Y. Lou, J. Chen, Y. Yang, W.W. Overwijk, L. Radvanyi
Analysis and interpretation of data (e.g., statistical analysis, biostatistics, computational analysis): W. Peng, C. Liu, G. Lizee, L. Radvanyi
Writing, review, and/or revision of the manuscript: W. Peng, C. Liu, H. Yagita, W.W. Overwijk, G. Lizee, P. Hwu
Administrative, technical, or material support (i.e., reporting or organizing data, constructing databases): W. Peng, C. Liu, Y. Lou, Y. Yang, H. Yagita, P. Hwu
Study supervision: L. Radvanyi, P. Hwu

References

1. Peddareddigari VR, Miller PW, Nebiyou BB, Overwijk WW, Ross MI, Lee JE, et al. Effect of clinical status and previous treatment of melanoma patients on expansion of TIL for adoptive T-cell therapy. ASCO Meeting Abstracts 2009;27:3021.
2. Pule MA, Savoldo B, Myers GD, Rossig C, Russell HV, Dotti G, et al. Virus-specific T cells engineered to coexpress tumor-specific receptors: persistence and antitumor activity in individuals with neuroblastoma. Nat Med 2008;14:1264–70.
3. Porter DL, Levine BL, Kalos M, Bagg A, June CH. Chimeric antigen receptor-modified T cells in chronic lymphoid leukemia. N Engl J Med 2011;365:725–33.
4. Laszlo G, Radvanyi CB, Minying Zhang, Priscilla Miller MG, Nicholas Papadopoulos, Patrick Hwu. Adoptive T cell therapy for metastatic melanoma: the MD Anderson experience. J Immunother 2010;33:863.
5. Fisher B, Packard BS, Read EJ, Carrasquillo JA, Carter CS, Topalian SL, et al. Tumor localization of adoptively transferred indium-111 labeled tumor infiltrating lymphocytes in patients with metastatic melanoma. J Clin Oncol 1989;7:250–61.
6. Griffith KD, Read EJ, Carrasquillo JA, Carter CS, Yang JC, Fisher B, et al. *In vivo* distribution of adoptively transferred indium-111-labeled tumor infiltrating lymphocytes and peripheral blood lymphocytes in patients with metastatic melanoma. J Natl Cancer Inst 1989;81:1709–17.
7. Lizee G, Radvanyi LG, Overwijk WW, Hwu P. Improving antitumor immune responses by circumventing immunoregulatory cells and mechanisms. Clin Cancer Res 2006;12:4794–803.
8. Hawkins RE, Gilham DE, Debets R, Eshhar Z, Taylor N, Abken H, et al. Development of adoptive cell therapy for cancer: a clinical perspective. Hum Gene Ther 2010;21:665–72.
9. Peng W, Ye Y, Rabinovich BA, Liu C, Lou Y, Zhang M, et al. Transduction of tumor-specific T cells with CXCR2 chemokine receptor improves migration to tumor and antitumor immune responses. Clin Cancer Res 2010;16:5458–68.
10. Heemskerk B, Liu K, Dudley ME, Johnson LA, Kaiser A, Downey S, et al. Adoptive cell therapy for patients with melanoma, using tumor-infiltrating lymphocytes genetically engineered to secrete interleukin-2. Hum Gene Ther 2008;19:496–510.
11. Till BG, Jensen MC, Wang J, Chen EY, Wood BL, Greisman HA, et al. Adoptive immunotherapy for indolent non-Hodgkin lymphoma and mantle cell lymphoma using genetically modified autologous CD20-specific T cells. Blood 2008;112:2261–71.
12. Fife BT, Pauken KE. The role of the PD-1 pathway in autoimmunity and peripheral tolerance. Ann N Y Acad Sci 2011;1217:45–59.
13. Parry RV, Chemnitz JM, Frauwirth KA, Lanfranco AR, Braunstein I, Kobayashi SV, et al. CTLA-4 and PD-1 receptors inhibit T-cell activation by distinct mechanisms. Mol Cell Biol 2005;25:9543–53.
14. Blank C, Brown I, Peterson AC, Spiotto M, Iwai Y, Honjo T, et al. PD-L1/B7H-1 inhibits the effector phase of tumor rejection by T cell receptor (TCR) transgenic CD8+ T cells. Cancer Res 2004;64:1140–5.
15. Blank C, Gajewski TF, Mackensen A. Interaction of PD-L1 on tumor cells with PD-1 on tumor-specific T cells as a mechanism of immune evasion: implications for tumor immunotherapy. Cancer Immunol Immunother 2005;54:307–14.
16. Yamazaki T, Akiba H, Koyanagi A, Azuma M, Yagita H, Okumura K. Blockade of B7-H1 on macrophages suppresses CD4+ T cell proliferation by augmenting IFN-gamma-induced nitric oxide production. J Immunol 2005;175:1586–92.
17. Curran MA, Montalvo W, Yagita H, Allison JP. PD-1 and CTLA-4 combination blockade expands infiltrating T cells and reduces regulatory T and myeloid cells within B16 melanoma tumors. Proc Natl Acad Sci U S A 2010;107:4275–80.
18. Ishida Y, Agata Y, Shibahara K, Honjo T. Induced expression of PD-1, a novel member of the immunoglobulin gene superfamily, upon programmed cell death. EMBO J 1992;11:3887–95.
19. Barber DL, Wherry EJ, Masopust D, Zhu B, Allison JP, Sharpe AH, et al. Restoring function in exhausted CD8 T cells during chronic viral infection. Nature 2006;439:682–7.
20. Day CL, Kaufmann DE, Kiepiela P, Brown JA, Moodley ES, Reddy S, et al. PD-1 expression on HIV-specific T cells is associated with T-cell exhaustion and disease progression. Nature 2006;443:350–4.

21. Trautmann L, Janbazian L, Chomont N, Said EA, Gimmig S, Bessette B, et al. Upregulation of PD-1 expression on HIV-specific CD8+ T cells leads to reversible immune dysfunction. Nat Med 2006;12:1198–202.

22. Nishimura H, Nose M, Hiai H, Minato N, Honjo T. Development of lupus-like autoimmune diseases by disruption of the PD-1 gene encoding an ITIM motif-carrying immunoreceptor. Immunity 1999;11: 141–51.

23. Wang J, Yoshida T, Nakaki F, Hiai H, Okazaki T, Honjo T. Establishment of NOD-Pdcd1-/- mice as an efficient animal model of type I diabetes. Proc Natl Acad Sci U S A 2005;102:11823–8.

24. Zhang Y, Huang S, Gong D, Qin Y, Shen Q. Programmed death-1 upregulation is correlated with dysfunction of tumor-infiltrating CD8+ T lymphocytes in human non-small cell lung cancer. Cell Mol Immunol 2010;7:389–95.

25. Wang SF, Fouquet S, Chapon M, Salmon H, Regnier F, Labroquere K, et al. Early T cell signalling is reversibly altered in PD-1+ T lymphocytes infiltrating human tumors. PLoS One 2011;6:e17621.

26. Thompson RH, Dong H, Lohse CM, Leibovich BC, Blute ML, Cheville JC, et al. PD-1 is expressed by tumor-infiltrating immune cells and is associated with poor outcome for patients with renal cell carcinoma. Clin Cancer Res 2007;13:1757–61.

27. Chapon M, Randriamampita C, Maubec E, Badoual C, Fouquet S, Wang SF, et al. Progressive upregulation of PD-1 in primary and metastatic melanomas associated with blunted TCR signaling in infiltrating T lymphocytes. J Invest Dermatol 2011;131:1300–7.

28. Hino R, Kabashima K, Kato Y, Yagi H, Nakamura M, Honjo T, et al. Tumor cell expression of programmed cell death-1 ligand 1 is a prognostic factor for malignant melanoma. Cancer 2010;116:1757–66.

29. Karim R, Jordanova ES, Piersma SJ, Kenter GG, Chen L, Boer JM, et al. Tumor-expressed B7-H1 and B7-DC in relation to PD-1+ T-cell infiltration and survival of patients with cervical carcinoma. Clin Cancer Res 2009;15:6341–7.

30. Nomi T, Sho M, Akahori T, Hamada K, Kubo A, Kanehiro H, et al. Clinical significance and therapeutic potential of the programmed death-1 ligand/programmed death-1 pathway in human pancreatic cancer. Clin Cancer Res 2007;13:2151–7.

31. Thompson RH, Gillett MD, Cheville JC, Lohse CM, Dong H, Webster WS, et al. Costimulatory B7-H1 in renal cell carcinoma patients: indicator of tumor aggressiveness and potential therapeutic target. Proc Natl Acad Sci U S A 2004;101:17174–9.

32. Zhou Q, Xiao H, Liu Y, Peng Y, Hong Y, Yagita H, et al. Blockade of programmed death-1 pathway rescues the effector function of tumor-infiltrating T cells and enhances the antitumor efficacy of lentivector immunization. J Immunol 2010;185:5082–92.

33. Brahmer JR, Drake CG, Wollner I, Powderly JD, Picus J, Sharfman WH, et al. Phase I study of single-agent anti-programmed death-1 (MDX-1106) in refractory solid tumors: safety, clinical activity, pharmacodynamics, and immunologic correlates. J Clin Oncol 2010;28:3167–75.

34. Topalian SL, Hodi FS, Brahmer JR, Gettinger SN, Smith DC, McDermott DF, et al. Safety, activity, and immune correlates of anti-PD-1 antibody in cancer. N Engl J Med 2012;36:2443–54.

35. Berger R, Rotem-Yehudar R, Slama G, Landes S, Kneller A, Leiba M, et al. Phase I safety and pharmacokinetic study of CT-011, a humanized antibody interacting with PD-1, in patients with advanced hematologic malignancies. Clin Cancer Res 2008;14:3044–51.

36. Mkrtichyan M, Najjar YG, Raulfs EC, Abdalla MY, Samara R, Rotem-Yehudar R, et al. Anti-PD-1 synergizes with cyclophosphamide to induce potent anti-tumor vaccine effects through novel mechanisms. Eur J Immunol 2011;41:2977–86.

37. Sierro SR, Donda A, Perret R, Guillaume P, Yagita H, Levy F, et al. Combination of lentivector immunization and low-dose chemotherapy or PD-1/PD-L1 blocking primes self-reactive T cells and induces anti-tumor immunity. Eur J Immunol 2011;41:2217–28.

38. Agata Y, Kawasaki A, Nishimura H, Ishida Y, Tsubata T, Yagita H, et al. Expression of the PD-1 antigen on the surface of stimulated mouse T and B lymphocytes. Int Immunol 1996;8:765–72.

39. Zhang M, Maiti S, Bernatchez C, Huls H, Rabinovich BA, Champlin RE, et al. A new approach to simultaneously quantify both TCR alpha- and beta-chain diversity after adoptive immunotherapy. Clin Cancer Res 2012;18:4733–42.

40. Luster AD, Ravetch JV. Biochemical characterization of a gamma interferon-inducible cytokine (IP-10). J Exp Med 1987;166:1084–97.

Cancer Research

PD-1 Blockade Enhances T-cell Migration to Tumors by Elevating IFN- γ Inducible Chemokines

Weiyi Peng, Chengwen Liu, Chunyu Xu, et al.

Updated version	Access the most recent version of this article at: doi:10.1158/0008-5472.CAN-12-1187
Supplementary Material	Access the most recent supplemental material at: http://cancerres.aacrjournals.org/content/suppl/2012/08/20/0008-5472.CAN-12-1187.DC1

Cited articles	This article cites 40 articles, 19 of which you can access for free at: http://cancerres.aacrjournals.org/content/72/20/5209.full#ref-list-1
Citing articles	This article has been cited by 38 HighWire-hosted articles. Access the articles at: http://cancerres.aacrjournals.org/content/72/20/5209.full#related-urls

E-mail alerts	Sign up to receive free email-alerts related to this article or journal.
Reprints and Subscriptions	To order reprints of this article or to subscribe to the journal, contact the AACR Publications Department at pubs@aacr.org.
Permissions	To request permission to re-use all or part of this article, use this link http://cancerres.aacrjournals.org/content/72/20/5209. Click on "Request Permissions" which will take you to the Copyright Clearance Center's (CCC) Rightslink site.